damaged lung [24], while IFN-γ works as a key cytokine in protective cellular immunity against *Legionella* [25]. These cytokines might demonstrate different *in vivo* kinetics although both cytokines are thought to play a significant role in *Legionella* pneumonia.

This study was retrospective and had several limitations. Firstly, the number of BA samples was relatively small, because *Legionella* pneumonia cases were not so many diagnosed before bronchoscopic examination, and the collection and appropriate stock of the BA samples were not always performed. The measurements of BA fluids did not include control subjects for ethical limitation of this study. Instead, we compared the concentration of cytokines in BA fluids with those in the sera of identical patients. Secondly, serum HMGB-1 was determined in single point when the pneumonia was diagnosed. Kinetic study of serum HMGB-1 may demonstrate significant increase of the cytokine during the course of disease. Even with these limitations, this study demonstrates novel finding on role of HMGB-1 in severe *Legionella* pneumonia. It is also noted that the finding may not be specific to *Legionella* pneumonia.

In conclusion, the levels of HMGB-1 and other cytokines, including HGF and IFN-γ were elevated in the BA fluids of patients with *Legionella* pneumonia, while serum HMGB-1 was not significantly elevated. The present findings suggest significant role of intra-pulmonary HMGB-1 in severe pneumonia due to *Legionella* spp. Further studies are warranted to identify the role of HMGB-1 in severe pneumonia caused by various respiratory pathogens.

Conflict of interest

None.

References

[1] Edelstein PH, Cianciotto NP. Legionella. In: Mandell GL, Bennett JE, Dolin R, editors. Principles and practice of infectious diseases. 7th ed. Philadelphia, PA: Elsevier Churchill Livingstone; 2010. pp. 2711–24.
[2] Ciloniz C, Ewig S, Polverino E, Marcos MA, Esquinas C, Gabarrus A, et al. Microbial aetiology of community-acquired pneumonia and its relation to severity. Thorax 2011;66:340–6.
[3] Arancibia R, Cortes CP, Valdes M, Cerda J, Hernandez A, Soto L, et al. Importance of *Legionella pneumophila* in the etiology of severe community-acquired pneumonia in Santiago, Chile. Chest 2013 June 13 [ePub ahead of print].
[4] Valles J, Mesalles E, Mariscal D, Fernandez M, Pena R, Jimenez JL, et al. A 7-year study of severe hospital-acquired pneumonia requiring ICU. Intensive Care Med 2003;29:1981–8.
[5] Demello D, Kierol-Andrew L, Scalise FJ. Severe sepsis and acute respiratory distress syndrome from community-acquired *Legionella pneumophila* pneumonia: case report. Am J Crit Care 2007;16:320.
[6] Kakeya H, Ehara N, Fukushima K, Seki M, Izumikawa K, Yamamoto Y, et al. Severe Legionnaires' disease successfully treated using a combination of fluoroquinolone, erythromycin, corticosteroid, and sivelestat. Intern Med 2008;47:773–7.
[7] Liu Y, Prasad R, Wilson SH. HMGB1: roles in base excision repair and related function. Biochim Biophys Acta 2010;1799:119–30.
[8] Sunden-Cullberg J, Norrby-Teglund A, Treutiger CJ. The role of high mobility group box-1 protein in severe sepsis. Curr Opin Infect Dis 2006;19:231–6.
[9] Ueno H, Matsuda T, Hashimoto S, Amaya F, Kitamura Y, Tanaka M, et al. Contributions of high mobility group box protein in experimental and clinical acute lung injury. Am J Respir Crit Care Med 2004;170:1310–6.
[10] Furugen M, Higa F, Hibiya K, Teruya H, Akamine M, Haranaga S, et al. *Legionella pneumophila* infection induces programmed cell death, caspases activation, and release of high mobility group box 1 protein in A549 alveolar epithelial cells. Respir Res 2007;9:39.
[11] Morinaga Y, Yanagihara K, Nakamura S, Hasegawa H, Seki M, Izumikawa K, et al. *Legionella pneumophila* induces cathepsin B-dependent necrotic cell death with releasing high mobility group box1 in macrophages. Respir Res 2010;11:158.
[12] Fine MJ, Auble TE, Yealy DM, Hanusa BH, Weissfeld LA, Singer DE, et al. A prediction rule to identify low risk patients with community-acquired pneumonia. N Engl J Med 1997;336:243–50.
[13] Yamada S, Yakabe K, Ishii J, Imaizumi H, Maruyama I. New high mobility group box 1 assay system. Clin Chim Acta 2006;372:173–8.
[14] van Zoelen MAD, Laterre P-F, van Veen SQ, van Till JWO, Wittebole X, Bresser P, et al. Systemic and local high mobility group box 1 concentrations during severe infection. Crit Care Med 2007;35:2799–804.
[15] Gaïni S, Pedersen SS, Koldkjaer OG, Pedersen C, Møller HJ. High mobility group box-1 protein in patients with suspected community- acquired infections and sepsis: a prospective study. Crit Care 2007;11:R32.
[16] Angus DC, Yang L, Kong L, Kellum JA, Delude RL, Tracey KJ, et al. Circulating high-mobility group box 1 (HMGB1) concentrations are elevated in both uncomplicated pneumonia and pneumonia with severe sepsis. Crit Care Med 2007;35:1061–7.
[17] Tabata C, Shibata E, Tabata R, Kanemura S, Mikami K, Nogi Y, et al. Serum HMGB1 as a prognostic marker for malignant pleural mesothelioma. BMC Cancer 2013;13:205.
[18] Lee H, Song M, Shin N, Shin CH, Min BS, Kim H, et al. Diagnostic significance of serum HMGB1 in colorectal carcinomas. PLos One 2012;7:e34318.
[19] Majumdar M, Ratho R, Chawla Y, Singh MP. High levels of circulating HMGB1 as a biomarker of acute liver failure in patients with viral hepatitis E. Liver Int 2013;33:1341–8.
[20] Bruchfeld A, Qureshi AR, Lindholm B, Barany P, Yang L, Stenvinkel P, et al. High mobility group box protein-1 correlates with renal function in chronic kidney disease (CKD). Mol Med 2008;14:109–15.
[21] Ogawa EN, Ishizaka A, Tasaka S, Koh H, Ueno H, Amaya F, et al. Contribution of high-mobility group box-1 to the development of ventilator-induced lung injury. Am J Respir Crit Care Med 2006;174:400–7.
[22] Higa F, Akamine M, Furugen M, Hibiya K, Koide M, Tamayose M, et al. Hepatocyte growth factor levels in *Legionella* pneumonia: a retrospective study. BMC Infect Dis 2011;11:74.
[23] Tateda K, Matsumoto T, Ishii Y, Furuya N, Ohno A, Miyazaki S, et al. Serum cytokines in patients with *Legionella* pneumonia: relative predominance of Th1-type cytokines. Clin Diagn Lab Immunol 1998;5:401–3.
[24] Crestani B, Marchand-Adam S, Quesnel C, Plantier L, Borensztajn K, Marchal J, et al. Hepatocyte growth factor and lung fibrosis. Proc Am Thorac Soc 2012;9:158–63.
[25] Nash TW, Libby DM, Horwitz MA. IFN-gamma-activated human alveolar macrophages inhibit the intracellular multiplication of *Legionella pneumophila*. J Immunol 1988;140:3978–81.

INTERNAL MEDICINE

□ ORIGINAL ARTICLE □

Clinicopathological Findings of Four Cases of Pure Influenza Virus A Pneumonia

Jiro Fujita[1], Yuji Ohtsuki[2], Hajime Higa[3], Masato Azuma[3], Takeo Yoshinouchi[4], Shusaku Haranaga[1], Futoshi Higa[1] and Masao Tateyama[1]

Abstract

Objective The purpose of this study was to perform clinicopathological evaluations of patients with pure influenza A virus pneumonia.

Methods We performed clinicopathological analyses of four cases of pure influenza A virus pneumonia.

Patients Among the four cases, three were caused by the pandemic (H1N1) 2009 virus. Three patients were analyzed during autopsy, and one underwent transbronchial lung biopsy.

Results We suggest that the interval between influenza virus A pneumonia onset and our analysis affected the pathological findings. Diffuse alveolar damage was observed during the acute phase. After ten days, organizing pneumonia and marked proliferation of premature type II alveolar epithelium were observed. Clinically, intra-alveolar hemorrhage was observed in two patients. Pathologically, hyaline membrane formation and intra-alveolar hemorrhage were observed in all cases.

Conclusion Severe epithelial damage was determined as the main mechanism of respiratory failure caused by influenza A virus pneumonia.

Key words: influenza A virus, pneumonia, diffuse alveolar damage, alveolar hemorrhage, organizing pneumonia

(Intern Med 53: 1333-1342, 2014)
(DOI: 10.2169/internalmedicine.53.1174)

Introduction

Influenza virus is a common cause of lower respiratory tract infections in adults. Infections can occur as pandemics, epidemics, or sporadic outbreaks. Clinical pneumonia attributable to influenza virus infection is uncommon, but when it does occur, secondary bacterial pneumonia, as well as pure influenza viral pneumonia, need to be considered as possible causes. Pure influenza viral pneumonia can be overwhelming in some patients and can result in death within 24 hours of onset.

A pandemic caused by the pandemic (H1N1) 2009 virus occurred during the 2009/2010 influenza seasons. Many reports described pathological findings of pneumonia caused by pandemic (H1N1) 2009 virus; however, few studies clinicopathologically evaluated lung specimens.

The aim of the present study was to describe the clinicopathological findings of three autopsied cases and one survived case of influenza A virus pneumonia. We herein demonstrate that hyaline membrane formation and pulmonary hemorrhage play significant roles in the pathogenesis of pure influenza A virus pneumonia.

Materials and Methods

The four cases are described in Table 1. Three patients died more than 10 days from influenza A virus pneumonia onset. In cases 2, 3, and 4, extracorporeal membrane oxygenation (ECMO) was used to control respiratory failure.

[1]Department of Infectious, Respiratory, and Digestive Medicine, Control and Prevention of Infectious Diseases (The First Department of Internal Medicine), Faculty of Medicine, University of the Ryukyus, Japan, [2]Division of Pathology, Matsuyama Shimin Hospital, Japan, [3]Department of Internal Medicine, Okinawa Prefectural Nanbu Medical Center, Japan and [4]Department of Internal Medicine, Toyokawa Municipal Hospital, Japan

Received for publication June 18, 2013; Accepted for publication January 26, 2014

Correspondence to Dr. Jiro Fujita, fujita@med.u-ryukyu.ac.jp

Table 1. Clinicopathological Features of 4 Cases of Pure Influenza Pneumonia

Case	Age & Sex	Sick contact/Smoking/Season/ Underlying diseases/Cardiovasucular test (Echo)	Chest X-ray	Chest CT	Color of BAL fluids	Clinical diagnosis	Virus	The interval between onset and pathological analysis	Anti-influenza drugs/Antibiotics/Clinical resoponse	Main pathological findings	Outcome
1	97 female	None/None/December/Diabetes/Unknown	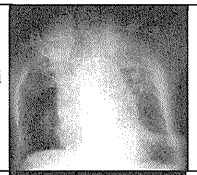	Not examined	Not examined	ARDS	A	12	none/+(unknown)/poor	Diffuse alveolar damage with pulmonary hemorrhage, bronchiolitis, and organizing pneumonia	Dead
2*	24 female	Yes/None/August/Mental retardation/Normal	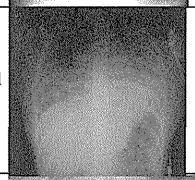	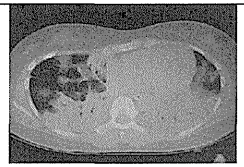	Not examined	ARDS	pdmH1N1	16	oseltamivir/meropenem+vancomycin/poor	Diffuse alveolar damage with the marked proliferation of pleomorphic type II alveolar epithelium, and organizing pneumonia	Dead
3	59 male	None/Yes/January/Obesity/Normal	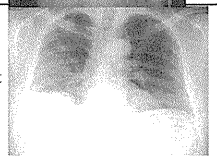	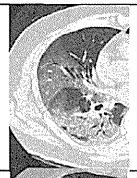		ARDS	pdmH1N1	1	peramivir/none/poor	Diffuse alveolar damage	Alive
4	37 male	Yes/Unknown/January/Obesity/Normal	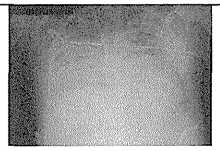	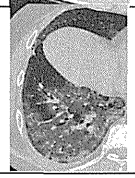		ARDS	pdmH1N1	15	laninamivir→ oseltamivir/cefotaxime+azithromycin/poor	Pulmonary hemorrhage and edema, and organizing pneumonia	Dead

*see reference 25

Intern Med 53: 1333-1342, 2014 DOI: 10.2169/internalmedicine.53.1174

Table 2. Summary of Histopathological Findings in Four Cases of Influenza Pneumonia

Findings/case#	Case 1	Case 2	Case 3	Case 4
Diffuse alveolar damage	3+	3+	2+	-
Hyaline membrane	3+	1+	2+	1+
Alveolar hemorrhage	2+	1+	1+	3+
Organizing pneumonia	3+	-	-	3+
Fibrin exudation	3+	-	-	1+
Myofibroblast proliferation	1+	-	-	3+
Thickening of alveolar orifices	3+	3+	-	-
Edema	3+	2+	-	2+
Bronchiolitis	3+	-	-	1+
Hemorrhage	3+	-	-	1+
Necrotic debris	3+	-	-	-

3+: frequently, 2+: sometimes, 1+: only focal, -: none

All three of these patients were diagnosed with pure influenza viral pneumonia and not secondary bacterial pneumonia based on the following evidence: i) the presence of infiltrates on chest radiographs and chest computed tomography (CT) scans; ii) influenza virus A infection was confirmed by a rapid diagnosis kit, as well as reverse transcriptase polymerase chain reaction (RT-PCR) for pandemic (H1N1) 2009; and iii) the absence of significant bacterial infection confirmed by repeated Gram stains and bacterial cultures.

As cases 2, 3, and 4 were infected with pandemic (H1N1) 2009 virus, RT-PCR was performed according to the guidelines of the National Institute of Infectious Diseases (Japan) for pandemic (H1N1) 2009 virus detection, and testing was undertaken at the Okinawa Prefectural Institute of Health and Environment.

Case 1

A 97-year-old woman was admitted to hospital because of low-grade fever and general fatigue. Her chest X-ray revealed infiltration in both lung fields. Her condition rapidly deteriorated and she died of respiratory failure on day 12. She was diagnosed to have influenza viral pneumonia based on the significant elevation of anti-influenza A antibody. An autopsy was performed. Evaluation of paired sera demonstrated that the titer of serum anti-influenza A antibody was significantly increased. A rapid antigen test was not performed.

Case 2

A 24-year-old woman with mental retardation had symptoms of fever and dry cough. A rapid diagnostic test for influenza using a throat swab was performed at an outpatient clinic, and it yielded positive results for influenza A antigen. Five days later, the patient developed further symptoms of persistent fever and dyspnea; she was diagnosed with severe pneumonia and was admitted to the hospital.

She developed respiratory failure, and mechanical ventilation was performed from admission to the time of death (16 days). In addition, ECMO was performed from days 2 to 12. After this treatment, chest X-rays taken at day 16 showed slight improvement of consolidation; however, the patient died due to a subarachnoid hemorrhage.

Case 3

A 59-year-old man who had no underlying diseases except for obesity was referred to a private clinic with a fever and a sore throat. A rapid diagnostic test for influenza using a throat swab was performed and was negative. His symptoms did not improve, and he developed dyspnea and inspiratory crackles in both lung fields, so he was transferred to a medium-sized hospital.

The patient was considered to have acute interstitial pneumonia based on chest radiological findings, and bronchoalveolar lavage (BAL) and transbronchial lung biopsy (TBLB) were performed. PCR of his BAL fluid for pandemic (H1N1) 2009 virus was positive.

Case 4

A 37-year-old man who had no underlying diseases except for obesity (body mass index of 33) was referred to a private clinic with a fever and a productive cough. A rapid diagnostic test for influenza using a throat swab was performed, and the result was negative. His symptoms did not improve, and he developed dyspnea and inspiratory crackles in both lung fields, so he was transferred to a medium-sized hospital.

The patient was considered to have acute interstitial pneumonia based on chest radiological findings, and BAL was performed. The BAL fluid was subjected to PCR for pandemic (H1N1) 2009 virus, which was positive. Mechanical ventilation was performed from days 7 to 15 for respiratory failure. ECMO was also performed from days 7 to 15. However, his respiratory condition deteriorated, and he died from respiratory failure.

Pathological analysis

In addition to Hematoxylin and Eosin (HE) staining, an Azan stain for collagen fibers and an Elastica van Gieson (EVG) stain for elastic fibers were also performed on tissue sections. Immunohistochemical stains used the avidin-biotin peroxidase complex (ABC) method (LSAB kit; Dako, Glostrup, Denmark) using the following antibodies: KL-6 [1:2,860, no pretreatment (NP), provided by Eisai Co., Tokyo, Japan], surfactant protein (SP)-A [1:100, autoclaving (AC), Dako], epithelial membrane antigen (EMA) [1:50, microwave (MW), Dako], factor VIII (1:400, NP; Dako), thyroid transcription factor-1 (TTF-1) (1:50, AC, Dako), AE1/AE3 [1:400, pronase (P); Boehringer-Mannheim Corp., Indianapolis, USA], h-caldesmon (1:50, AC; Lab Vision Corp. Fremont, USA), desmin (1:50, NP; Dako), and α-smooth muscle actin (SMA) (1:50, P; Becton-Dickinson, San Jose, USA). After confirming the specificity of these antibodies, the appropriate positive and negative controls were stained in parallel. All staining procedures were performed according to the manufacturers' instructions.

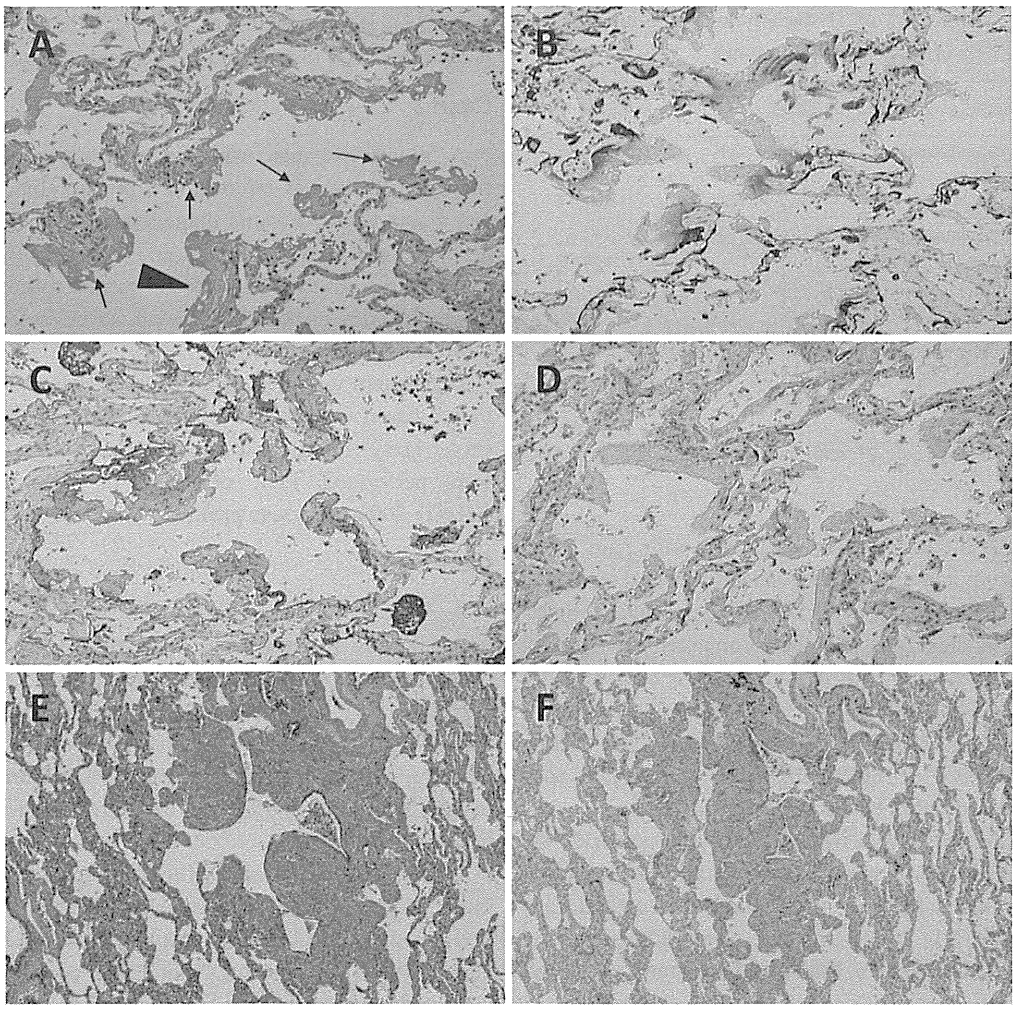

Figure 1. Pathological findings of case 1. (A) Hematoxylin and Eosin (H&E) staining showing alveolar epithelial cell damage at the alveolar orifices and irregular fragmented hyaline membranes. (B) Immunohistochemical staining with anti-AE1/AE3 antibody. Due to the alveolar epithelial cell damage, cytokeratin components are included in the hyaline membrane. Stronger staining was observed at the interstitium, and weaker staining was noted at the alveolar lumina. (C) Immunohistochemical staining with an anti-SP-A antibody. Most hyaline membranes are positive for the SP-A antibody. (D) Immunohistochemical staining with an anti-KL-6 antibody. The remaining alveolar epithelial cells were linearly stained with an anti-KL-6 antibody, but the hyaline membranes were negative. (E) Inner cavities of the respiratory bronchioles and alveolar ducts were narrowed and distorted. (F) Immunohistochemical staining with an anti-desmin antibody. Proliferated smooth muscle cells stained with an anti-desmin antibody were observed around the respiratory bronchioles and alveolar ducts. A, E: H&E staining, B-D, F: Labeled streptoavidin-biotin complex (LSABC) method, A-E: ×100, F: ×40.

Literature review

We reviewed the pertinent literature concerning pathological findings of pandemic (H1N1) 2009 virus pneumonia using Medline.

Results

Pathological analysis

There were heterogeneous pathological findings in these four cases (Table 2). The most significant findings were hyaline membrane formation and alveolar hemorrhage.

In case 1, the main pathological findings were bronchiolitis with hemorrhage and necrotic debris, diffuse alveolar

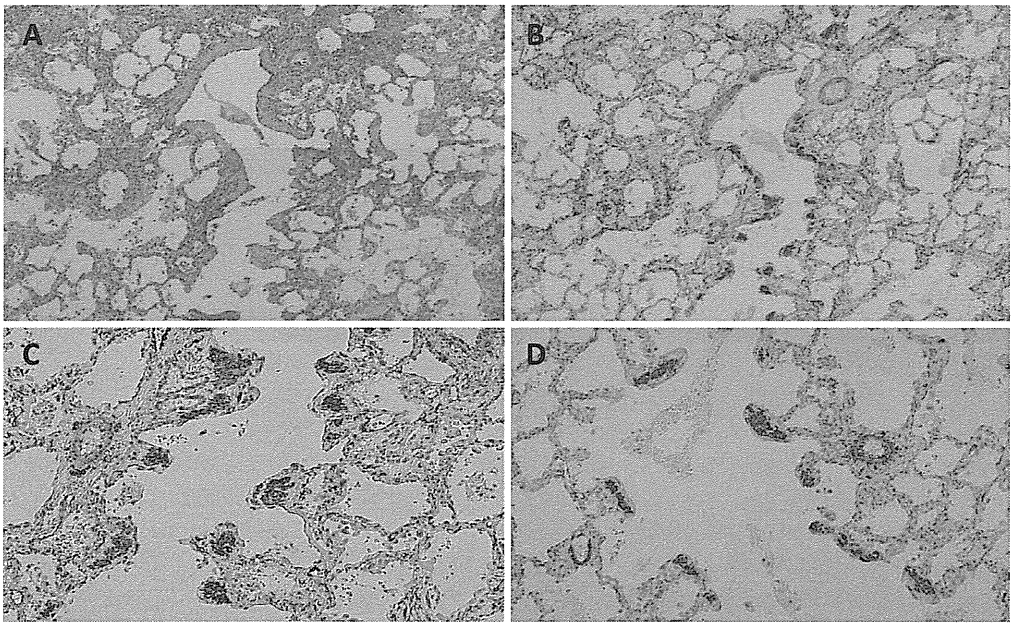

Figure 2. Pathological findings of case 2. (A) Hematoxylin and Eosin (H&E) staining. The respiratory bronchioles and alveolar ducts were markedly dilatated. (B) Immunohistochemical staining using an anti-α-SMA antibody. Small nodular foci of smooth muscle cells were positive for an anti-α-SMA antibody along with the alveolar ducts. (C) Immunohistochemical staining using an anti-α-SMA antibody. Nodular shaped proliferations are shown at higher magnification. (D) Immunohistochemical staining using an anti-caldesmon antibody. Nodular (C) and plate-like (D) proliferations of smooth muscle cells were observed just beneath the alveolar epithelium at the location of the alveolar orifices. A: H&E staining, B-D: LSABC method, A, B: ×40, C, D: ×100.

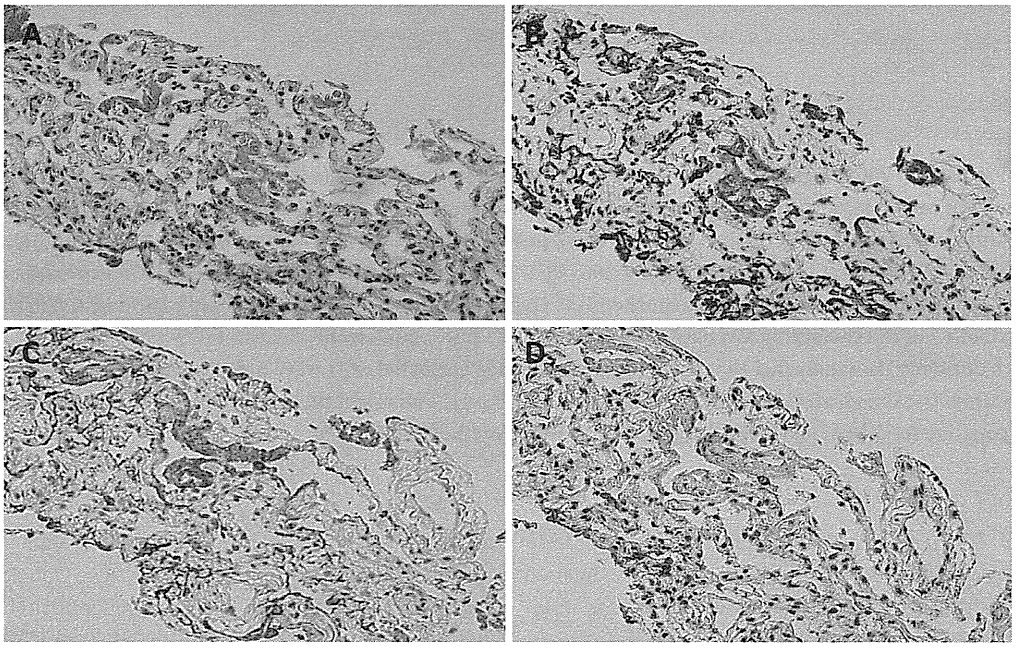

Figure 3. Pathological findings of case 3. (A) Hematoxylin and Eosin (H&E) staining showing hyaline membrane formation. (B) Immunohistochemical staining using an anti-AE1/AE3 antibody. Due to alveolar epithelial cell damage, cytokeratin was present in the hyaline membrane. (C) Immunohistochemical staining using an anti-EMA antibody showing weak hyaline membrane positivity and linear staining of the remaining alveolar epithelial cells. (D) Immunohistochemical staining using an anti-KL-6 antibody showed faint hyaline membrane labeling and associated linear staining of the remaining alveolar epithelial cells. A: H&E staining, B-D: LSABC method, A-D: ×200.

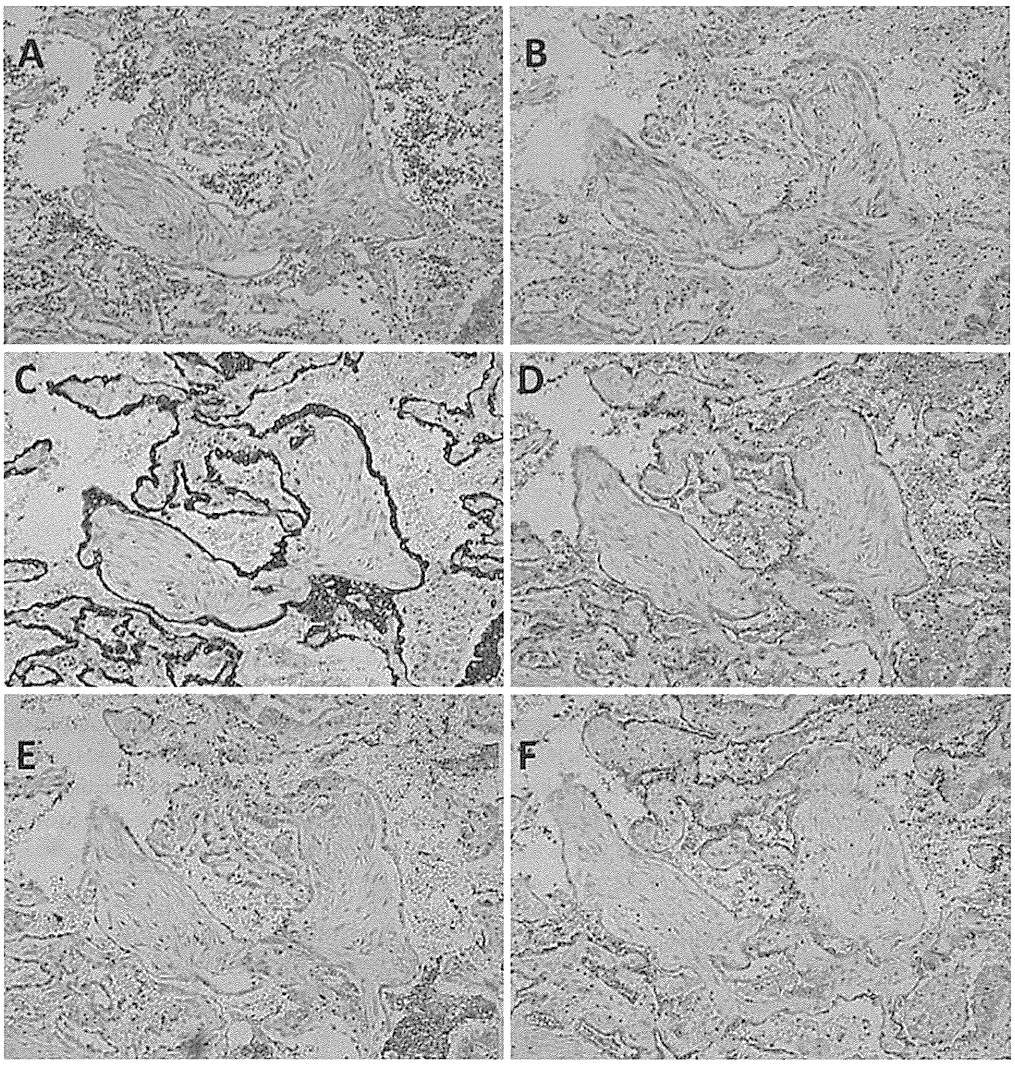

Figure 4. **Pathological findings of case 4. (A) Hematoxylin and Eosin (H&E) staining showing organizing pneumonia with intra-alveolar Masson's bodies. (B) Immunohistochemical staining using an anti-α-SMA antibody. Marked intra-alveolar proliferation of myofibroblasts was demonstrated. (C) Immunohistochemical staining with an anti-AE1/AE3 antibody revealed clear cytokeratin expression in epithelial cells. (D) Immunohistochemical staining with an anti-KL-6 antibody showed linearly staining of the remaining alveolar epithelial cells. (E) Immunohistochemical staining with an anti-SP-A antibody demonstrated that the remaining alveolar epithelial cells were negative for SP-A. (F) Immunohistochemical staining with an anti-EMA antibody. The remaining alveolar epithelial cells were negative for EMA. A: H&E staining, B-F: LSABC method. A-F: ×100.**

damage (DAD, Fig. 1A), and alveolar hemorrhage. In addition, organizing pneumonia with prominent fibrin exudation and pulmonary edema were also observed. Irregularly fragmented hyaline membranes were seen at the alveolar orifices (Fig. 1A). The hyaline membranes were stained with an anti-AE1/3 antibody (Fig. 1B) and an anti-SP-A antibody (Fig. 1C), suggesting that epithelial cell damage took place before formation of the hyaline membrane. In contrast, although remaining alveolar epithelial cells were linearly stained with an anti-KL-6 antibody, the hyaline membrane was not stained in this case (Fig. 1D). In addition, the remaining alveolar epithelial cells were linearly stained with an anti-EMA antibody, but hyaline membranes were focally stained. Hyaline membranes were also labeled with anti-factor VIII antibody. We observed subepithelial smooth muscle proliferations below the respiratory bronchioles (Fig. 1E) and narrowing of its inner space (Fig. 1F).

In case 2, lung specimens obtained by autopsy were diagnosed as being consistent with the organizing phase of DAD (Fig. 2A). In addition, marked nodular proliferation of smooth muscle cells was demonstrated at the location of alveolar orifices (Fig. 2A). Immunohistochemical staining using an anti-α-SMA antibody demonstrated marked smooth muscle cells proliferation at alveolar ducts (Fig. 2B). A

Table 3. Summary of Previous Studies Describing Pathological Analysis of Lung Specimens from Patients with H1N1 Influenza Infection

Reference	Patients	Pathological findings	Immunohistochemical analysis
1	Autopsied 1 case	Diffuse alveolar damage	Not done
2	77 cases	Bacterial coinfection	For pathogens
3	Autopsied 5 cases	Diffuse alveolar damage + superimposed bacterial infections	Not done
4	Autopsied 1 case	Diffuse alveolar damage	CD4, CD8, and influenza virus
5	Autopsied 1 case	Diffuse alveolar damage	Influenza virus
6	Open lung biopsied 5 cases and autopsied 1 case	Diffuse alveolar damage ± acute bacterial pneumonia	Not done
7	Autopsied 21 cases	Diffuse alveolar damage ± alveolar hemorrhage	Toll-like receptor-3, interferon-γ, tumor necrosis factor-α, CD8
8	Autopsied 34 cases	Diffuse alveolar damage ± superimposed bacterial infections	Influenza virus
9	Autopsied 2 cases	Acute and/or necrotizing pneumonia	Not done
10	Autopsied 100 cases	Diffuse alveolar damage ± bacterial co-	For pathogens
11	Autopsied 8 cases	Diffuse alveolar damage ± bacterial co-	Not done
12	Autopsied 1 case	Diffuse alveolar damage	Not done
13	Autopsied 1 case	Diffuse alveolar damage	Not done
14	Autopsied 8 cases	Tracheitis, necrotizing bronchiolitis, and alveolitis	Influenza virus
15	Autopsied 6 cases	Diffuse alveolar damage	Influenza virus
16	68 autopsy reports	Necrotizing bronchiolitis, diffuse alveolar damage, bacterial and fungal co-infection hemorrhage	Not done
17	5 open lung biopsy	Necrotizing bronchiolitis, diffuse alveolar damage, alveolar hemorrhage	CD68, CD4, CD8, CD20, NK, S100, IL-4, IL-10, iNOS
18	Autopsied 1 case	Diffuse alveolar damage, extensive intraalveolar haemorrhage	Not done
19	Autopsied 3 cases	Necrotizing bronchiolitis, epithelial necrosis and desquamation, and	Not done
20	Necropsied 5 cases	Diffuse alveolar damage	Influenza virus
21	Autopsied 20 cases	Viral infection in pneumocytes, which caused severe alveolar damage and fatal viral pneumonia	Influenza virus
22	Autopsied 6 cases	Diffuse alveolar damage in 5 cases and interstitial fibrosis in 1 case	Influenza virus
23	Autopsied 46 cases	Diffuse alveolar damage	Influenza virus
24	Autopsied 9 cases	Tracheitis, necrotizing bronchiolitis and diffuse alveolar damage	Influenza virus
25	Autopsied 1 case	Diffuse alveolar damage	Influenza A, AE1/AE3, CK19, CAM5.2, EMA, Alpha-SMA, SP-A, KL-6, TTF-1, Caldesmon, CD68, CD3, CD4, CD8, CD79a, MIB-1
26	Autopsied 1 case	Patchy necrotic foci with mononuclear inflammation in the lungs, myocarditis	Not done
27	Autopsied 8 cases	Diffuse alveolar damage accompanied by intraalveolar haemorrhage	AE1/AE3
28	Autopsied 21 case	Cellular localization of positive-stranded pH1N1 RNA in the lungs	Influenza virus

higher magnification of Fig. 2B revealed small nodular proliferation of smooth muscle cells (Fig. 2C). In addition, an anti-caldesmon antibody demonstrated plate-like proliferations of smooth muscle cells at the location of the alveolar orifices (Fig. 2D).

Case 3 was analyzed using specimens obtained by TBLB; therefore, bronchial lesions were not evaluated. However, this patient was evaluated at day 1, thus, DAD with hyaline membrane formation (Fig. 3A) as well as alveolar hemorrhage, representing the acute phase of DAD, were clearly observed. Hyaline membranes were stained with anti-AE1/3 (Fig. 3B) and anti-EMA (Fig. 3C) antibodies, suggesting that epithelial cell damage took place before formation of the hyaline membrane. In contrast, although the remaining alveolar epithelial cells were linearly stained with an anti-KL-6 antibody, the hyaline membrane was not (Fig. 3D). As shown in Table 1, the BAL fluid from this patient was reddish in color, suggesting that pulmonary hemorrhage had taken place, clinically as well as pathologically.

In case 4, although several pathological findings (alveolar hemorrhage and alveolar edema) were observed, the most prominent pathological feature was organizing pneumonia (Fig. 4A) with myofibroblast proliferation in Masson bodies (Fig. 4B). In addition, hyaline membranes were only rarely observed, suggesting that organizing pneumonia had occurred after epithelial cell damage. Alveolar duct dilatation and smooth muscle cell proliferation around the alveolar ducts were observed focally. Immunohistochemical staining

of Masson bodies using an anti-AE1/AE3 (pancytokeratin) antibody demonstrated continuous coverage by alveolar epithelial cells (Fig. 4C). Regenerated epithelial cells were linearly stained with an anti-KL-6 antibody (Fig. 4D). However, these cells were not stained with antibodies against SP-A (Fig. 4E), EMA (Fig. 4F), or TTF-1 (data not shown), suggesting that these epithelial cells were not mature. As shown in Table 1, the BAL fluid from this patient was red, therefore, pulmonary hemorrhage was demonstrated clinically and pathologically.

Literature review of literature

Our review of the literature revealed many autopsy studies of pandemic (H1N1) 2009 virus pneumonia (1-28, Table 3). The most prominent finding was DAD with or without pulmonary hemorrhage.

Discussion

Previously reported pathological findings of pneumonia caused by pandemic (H1N1) 2009 virus are presented in Table 3. In some cases, secondary bacterial pneumonia was observed. Many reports have pathologically analyzed lung specimens from patients with pandemic (H1N1) 2009 virus pneumonia and reported that DAD and alveolar hemorrhage were the predominant pathological features. However, immunohistochemical analyses have rarely been performed (4, 7, 17, 25, 27), and the precise mechanism of respiratory failure has not been demonstrated. In the present study, immunohistochemical analyses were also performed.

In the acute stage of influenza pneumonia as shown in case 3, although hyaline membrane formation was clearly observed, elastic fibers were not included in the hyaline membrane, suggesting that the architecture of the alveolar walls was preserved. It was possible to analyze the composition of the hyaline membranes in cases 1 and 3. In the hyaline membranes, pancytokeratin positivity exhibited gradation from the stromal site to the surface. In addition, hyaline membranes were also stained with anti-SP-A, anti-factor VIII, and anti-EMA antibodies, suggesting that epithelial cell damage took place before hyaline membrane formation. In contrast, the hyaline membrane was not stained with an anti-KL-6 antibody. Sun et al. reported that KL-6 positivity in the hyaline membrane (29); therefore, negative KL-6 staining in the hyaline membrane might be related to influenza A virus pneumonia.

Three of our cases were evaluated more than ten days after the onset of influenza A infection; therefore, several stages of regeneration were also observed. In case 1, organizing pneumonia with massive fibrin exudation was noted. In addition, organizing pneumonia with prominent myofibroblast proliferation was observed in case 4. Because case 3 experienced three cardiac arrests during his clinical course, no significant differences of backgrounds were observed among the medical histories of the four cases. All cases demonstrated very severe clinical courses.

Influenza A virus migrates from the upper respiratory tract and causes respiratory bronchiolitis; therefore, airway epithelial cells are significantly damaged. As shown in cases 1 and 2, prominent smooth muscle cell proliferation in the alveolar ducts seemed to be closely related to the airway epithelial cell damage. In addition, proliferation of subepithelial smooth muscle cells, which stained with anti-desmin antibody, was observed below the respiratory bronchioles, resulting in narrowing of the latter and reorganization of the alveolar structures. We suggest that this marked proliferation of smooth muscle cells might be related to the severe damage of the epithelial cells, as well as endothelial cells at the alveolar orifices.

In case 4, regenerated epithelial cells were linearly labeled with an anti-KL-6 antibody and partially stained with an anti-EMA antibody. They were negative for TTF-1 and SP-A, suggesting that these epithelial cells had characteristics of immature alveolar epithelium with no mitotic activity. These findings indicate that epithelial cell regeneration and maturation were important for recovery after epithelial cell damage; therefore, we suggest that absorption of organized tissue and maturation of epithelial cells were required to recover respiratory function.

Several reports have described pathological features in patients who died after a clinical course longer than ten days. Perez-Padilla et al. reported a 43-year-old patient who died after a 14-day illness complicated by acute renal failure and myocardial infection (1). Pathological evaluation of the lungs showed DAD, thick hyaline membranes, and prominent fibroblast proliferation. In addition, Harms et al. reported eight patients who died after illnesses >15 days, and organizing phases of DAD were observed in seven cases (87.5%) (11). However, they also found that only acute-phase DAD was observed in a 43-year-old man who died after a 27-day illness (11). Furthermore, Shelke et al. reported that lung specimens taken from patients who died within two weeks of symptom onset typically showed acute-phase DAD (23). In contrast, patients who died within three to four weeks of symptom onset showed both acute and organizing features, and the organizing and fibrotic stage of DAD was observed in patients who died after four weeks (23).

Influenza virus infection caused marked increases in the levels of pro-inflammatory cytokines, tumor necrosis factor-α, interleukin (IL)-6, and IL-1β (cytokine storm) (30). The inflammatory response also affected cell adhesion, vascular permeability, apoptosis, and mitochondrial reactive oxygen species, which could progress to vascular dysfunction and multi-organ failure. Studies have shown that influenza virus infection significantly upregulates the expression of cellular trypsins and matrix metalloproteinase-9 in various organs and vascular endothelial cells (30). We propose that in addition to direct damage to alveolar epithelial cells, cytokine storm-induced endothelial cell damage and successive vascular hyperpermeability play major roles in the pathogenesis of severe influenza virus-induced pneumonia.

It has been suggested that mechanical ventilation affects the pathological findings. Nakajima et al. reported that a 15-year-old boy who died after a 29-day illness and a 24-year-old woman who died after a 21-day illness showed extensive fibrosis. They also reported a 24-year-old woman who died after a 21-day illness who used ECMO from day seven onward, and the main pathological finding was organized DAD (21). In addition, Nin et al. described six autopsied cases and found that granulation tissue was present in four (8, 16, 36, and 45 days mechanical ventilation) (22). The patient with the longest time from diagnosis to death (45 days mechanical ventilation) had residual fibrosis with intense granulation tissue repair and interstitial inflammation. They concluded that signs of DAD evolved over time from exudative to proliferative and fibrotic changes according to the duration of mechanical ventilation (22).

The detection rate of influenza virus A changes according to disease duration. Shieh et al. reported 80 patients with known durations of illness (10). They showed positive immunohistochemistry for the influenza A viral antigen in respiratory tissues from 31 patients (39%) with illness duration less than ten days and in five patients (6%) with illness longer than ten days (10). In addition, Bhatnager et al. reported that none of their cases with long duration of illness (10-23 days) were positive by *in situ* hybridization, whereas all of them were positive by immunohistochemistry (28).

In the present study, immunohistochemical analysis was performed on autopsied lungs, and we found evidence of DAD caused by influenza pandemic (H1N1) 2009 virus infection. In cases 1 and 2, severe epithelial cell damage and marked proliferation of smooth muscle cells at the alveolar orifices were demonstrated. In addition, in cases 1 and 4, the organizing phase of DAD and type II alveolar cell regeneration were observed. However, regenerated type II cells did not entirely encompass the tip of the alveolar orifices. In addition, marked smooth muscle cell proliferation and increased collagen fibers were also seen in the subepithelial tissue at the alveolar orifices. The staining pattern of hyaline membranes suggested that the regenerated epithelial cells were immature and could not produce surfactant.

It is interesting that the hyaline membrane of patients with pure Influenza A pneumonia was negative for KL-6, and this should be investigated further. Sun et al. (29) reported that KL-6 expression is essential for the maturation of alveolar pneumocytes and that KL-6 expression proceeds linearly in alveolar pneumocytes from 23 weeks gestation. The findings from the present study suggest that the division and proliferation of type II pneumocytes, although frequently observed following epithelial cell damage caused by viral infection, fails to yield functionally mature cells that produce KL-6. This would explain the negative staining for KL-6 observed in the hyaline membrane. For cases 1, 2, and 4, the autopsies were performed more than ten days after the onset of influenza A infection, and the organization and proliferation of type II pneumocytes were observed in these specimens. Hence, the recovery of type II pneumocytes occurred prior to, or at approximately ten days post-infection. The absence of detectable KL-6 expression in these type II pneumocytes indicates that cell maturation was insufficient.

In conclusion, severe epithelial damage was determined to be the main mechanism of respiratory failure caused by influenza virus pneumonia.

The authors state that they have no Conflict of Interest (COI).

References

1. Perez-Padilla R, de la Rosa-Zamboni D, Ponce de Leon S, et al. Pneumonia and respiratory failure from swine-origin influenza A (H1N1) in Mexico. N Engl J Med **361**: 680-689, 2009.
2. Centers for Disease Control and Prevention (CDC). Bacterial coinfections in lung tissue specimens from fatal cases of 2009 pandemic influenza A (H1N1): United States, May-August 2009. Morb Mortal Wkly Rep **58**: 1071-1074, 2009.
3. Soto-Abraham MV, Soriano-Rosas J, Díaz-Quiñónez A, et al. Pathological changes associated with the 2009 H1N1 virus. N Engl J Med **361**: 2001-2003, 2009.
4. Takiyama A, Wang L, Tanino M, et al. Sudden death of a patient with pandemic influenza (A/H1N1pdm) virus infection by acute respiratory distress syndrome. Jpn J Infect Dis **63**: 72-74, 2010.
5. Nakajima N, Hata S, Sato Y, et al. The first autopsy case of pandemic influenza (A/H1N1pdm) virus infection in Japan: detection of a high copy number of the virus in type II alveolar epithelial cells by pathological and virological examination. Jpn J Infect Dis **63**: 67-71, 2010.
6. Gómez-Gómez A, Magaña-Aquino M, Garcia-Sepúlveda C, et al. Severe pneumonia associated with pandemic (H1N1) 2009 outbreak, San Luis Potosí, Mexico. Emerg Infect Dis **16**: 27-34, 2010.
7. Mauad T, Hajjar LA, Callegari GD, et al. Lung pathology in fatal novel human influenza A (H1N1) infection. Am J Respir Crit Care Med **181**: 72-79, 2010.
8. Gill JR, Sheng ZM, Ely SF, et al. Pulmonary pathologic findings of fatal 2009 pandemic influenza A/H1N1 viral infections. Arch Pathol Lab Med **134**: 235-243, 2010.
9. Murray RJ, Robinson JO, White JN, et al. Community-acquired pneumonia due to pandemic A (H1N1) 2009 influenza virus and methicillin resistant *Staphylococcus aureus* co-infection. PLoS One **5**: e8705, 2010.
10. Shieh WJ, Blau DM, Denison AM, et al. 2009 pandemic influenza A (H1N1): pathology and pathogenesis of 100 fatal cases in the United States. Am J Pathol **177**: 166-175, 2010.
11. Harms PW, Schmidt LA, Smith LB, et al. Autopsy findings in eight patients with fatal H1N1 influenza. Am J Clin Pathol **134**: 27-35, 2010.
12. Cunha BA, Syed U, Mickail N. Fulminant fatal swine influenza (H1N1): Myocarditis, myocardial infarction, or severe influenza pneumonia? Heart Lung **39**: 453-458, 2010.
13. Kling MC, Larian AA, Scordi-Bello I, Emer J, Lebwohl MG. Fatal influenza A(H1N1) respiratory tract infection in a patient having psoriasis treated with infliximab. Arch Dermatol **146**: 651-654, 2010.
14. Rosen DG, Lopez AE, Anzalone ML, et al. Postmortem findings in eight cases of influenza A/H1N1. Mod Pathol **23**: 1449-1457, 2010.
15. Calore EE, Uip DE, Perez NM. Pathology of the swine-origin influenza A (H1N1) flu. Pathol Res Pract **207**: 86-90, 2011.
16. Lucas S. Predictive clinicopathological features derived from systematic autopsy examination of patients who died with A/H1N1 influenza infection in the UK 2009-10 pandemic. Health Technol